http://dx.doi.org/10.5012/bkcs.2013.34.4.1081

Donor-π-Acceptor Type Diphenylaminothiophenyl Anthracene-mediated Organic Photosensitizers for Dye-sensitized Solar Cells

Dong Uk Heo, Sun Jae Kim, Beom Jin Yoo, Boeun Kim,† Min Jae Ko,† Min Ju Cho, and Dong Hoon Choi*

Department of Chemistry, Research Institute for Natural Sciences, Korea University, Seoul 136-701, Korea
**E-mail: dhchoi8803@korea.ac.kr*
†Photo-electronic Hybrids Research Center, Korea Institute of Science and Technology (KIST), Seoul 136-791, Korea
Received November 26, 2012, Accepted January 9, 2013

Two new metal-free organic dyes bridged by anthracene-mediated π-conjugated moieties were successfully synthesized for use in a dye-sensitized solar cell (DSSC). A *N,N*-diphenylthiophen-2-amine unit in these dyes acts as an electron donor, while a (*E*)-2-cyano-3-(thiophen-2-yl)acrylic acid group acts as an electron acceptor and an anchoring group to the TiO_2 electrode. The photovoltaic properties of (*E*)-2-cyano-3-(5-((10-(5-(diphenylamino)thiophen-2-yl)anthracen-9-yl)ethynyl)thiophen-2-yl)acrylic acid (DPATAT) and (*E*)-2-cyano-3-(5'-((10-(5-(diphenylamino)thiophen-2-yl)anthracen-9-yl)ethynyl)-2,2'-bithiophen-5-yl)acrylic acid (DPATABT) were investigated to identify the effect of conjugation length between electron donor and acceptor on the DSSC performance. By introducing an anthracene moiety into the dye structure, together with a triple bond and thiophene moieties for fine-tuning of molecular configurations and for broadening the absorption spectra, the short-circuit photocurrent densities (J_{sc}), and open-circuit photovoltages (V_{oc}) of DSSCs were improved. The improvement of J_{sc} in DSSC made of DPATABT might be attributed to much broader absorption spectrum and higher molecular extinction coefficient (ε) in the visible wavelength range. The DPATABT-based DSSC showed the highest power conversion efficiency (PCE) of 3.34% (η_{max} = 3.70%) under AM 1.5 illumination (100 mW cm^{-2}) in a photoactive area of 0.41 cm^2, with the J_{sc} of 7.89 mA cm^{-2}, the V_{oc} of 0.59 V, and the fill factor (*FF*) of 72%. In brief, the solar cell performance with DPATABT was found to be better than that of DPATAT-based DSSC.

Key Words : Dyes-sensitized solar cells, Anthracene, *N,N*-Diphenylthiophen-2-amine, Conjugation length, Power conversion efficiency

Introduction

Recently, dye-sensitized solar cells (DSSCs) have been highlighted because they are more efficient, cheaper, and facile to fabricate than conventional inorganic solar cells.[1,2] In a conventional electrochemical cell, Ru-complex photosensitizers such as N3 and N719 have exhibited power conversion efficiencies (PCEs) over ~12% under AM 1.5 irradiation,[3-5] whereas the solar cell made of organic photosensitizing dyes showed efficiencies around 6.5-9.0%.[6-10] Although the PCEs achieved with the metal-free organic dyes used in DSSCs are much lower than those achieved with Ru-based dyes, they also revealed many advantages over metal-containing dyes in DSSCs. It was suggested that metal-free organic dyes are environment friendly and have high molar extinction coefficients in a desired light wavelength range; further, flexibility of their molecular design and appropriate tuning of their molecular energy levels are advantageous to improve the PCEs in solar cells.

Promising organic photosensitizing dyes for DSSC have been reported recently, which contain indoline,[6] coumarin,[7,8] phenothiazine/phenoxazine,[9,10] merocyanine,[11,12] triarylamine,[13,14] and thiophene[15-20] units. According to most updated research, precisely designed metal-free organic dyes are able to be highly competitive candidates for use as photosensitizers in a highly efficient DSSC.

A common strategy for the design of highly efficient donor-π-acceptor (D-π-A) systems is the use of conjugated linking groups which can be tethered to the TiO_2 electrode as surface anchoring groups. Upon light irradiation, intramolecular photoinduced charge transfer from the donor to the acceptor is generated and a subsequent electron transfer to TiO_2 photoanode through the conjugated connecting group occurs. The preferential orientation of the dye on the TiO_2 surface not only improves donor ability at a distance from the photoinjected electrons, but also diminishes the detrimental impact of backward transfer of the electrons.

Simple 9,10-diaryl substituted anthracenes have been demonstrated as fluorescent materials while the incorporation of triarylamine moiety improves the hole-transporting ability of such compounds.[21-24] Even though the anthracene containing compounds have been developed successfully for applications to light-emitting diodes,[25-27] thin film transistors,[28-30] and bulk heterojunction solar cells[31] not much attempts was made to develop novel photosensitizers for fabricating high performance DSSC. Simple anthracene-mediated photosensitizers have been recently reported for DSSCs.[32-34] Hagfeldt *et al*.[32] employed anthracene unit as a conjugative linker for triphenylamine donor and cyanoacrylic acid acceptor. One of the dyes they synthesized

showed a prominent power conversion efficiency upto 7.03% under simulated AM 1.5 irradiation (100 mW/cm^2).

In this work, we demonstrated the synthesis of anthracene-mediated π-conjugated dyes for use in DSSCs. Thiophene and bithiophene units were introduced into 9,10-position of anthracene ring to steer the molecular structures of photosensitizing dyes and their molecular energy levels. The photovoltaic properties of DPATAT and DPATABT were measured to identify the effect of the conjugation length with thiophene and bithiophene conjugative linkers on the DSSC performance. In brief, the DSSC with DPATABT exhibited much better performance than the device with DPATABT due to more extended conjugation length and higher molar extinction coefficient (ε) in the wavelength range of solar emission.

Experimentals

Synthesis and Materials. All commercially available starting materials and solvents were purchased from Aldrich, TCI, and Acros Co. and used without further purification unless otherwise stated. HPLC grade toluene, acetonitrile, dimethylformamide (DMF), and tetrahydrofuran (THF) were purchased from Samchun Chemical and distilled from CaH_2 immediately before use. The intermediate compounds, **1**, **2**, and **5** were synthesized according to literature methods.[20(b),32,34]

5-((10-(5-(Diphenylamino)thiophen-2-yl)anthracen-9-yl)ethynyl)thiophene-2-carbaldehyde (3): Compound **1** (0.65 g, 1.66 mmol), compound **2** (0.689 g, 1.83 mmol), $Pd(PPh_3)_4$ (0.096 g, 0.083 mmol), K_2CO_3 (2.0 M, 15 mL), and Aliquat 336 (0.5 g) were dissolved in dried toluene (25 mL). The mixture was degassed and refluxed for 24 h under N_2 atmosphere. After cooling the mixture, the solvent was evaporated under vacuum and the crude product was extracted with methylene chloride (MC). After concentrating the mixture, silica-gel column chromatography employed to purify the crude product (MC: hexane (1:2 v/v)), gave pure

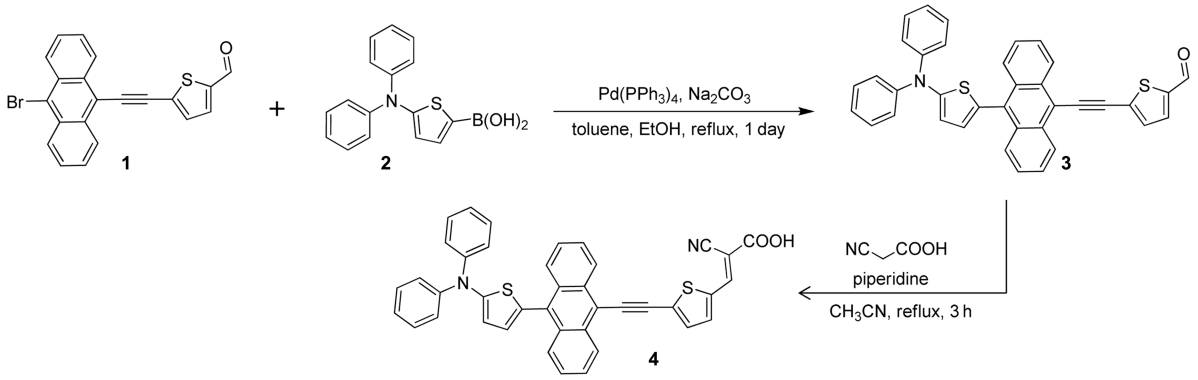

Scheme 1. Synthetic procedure for DPATAT, **4**.

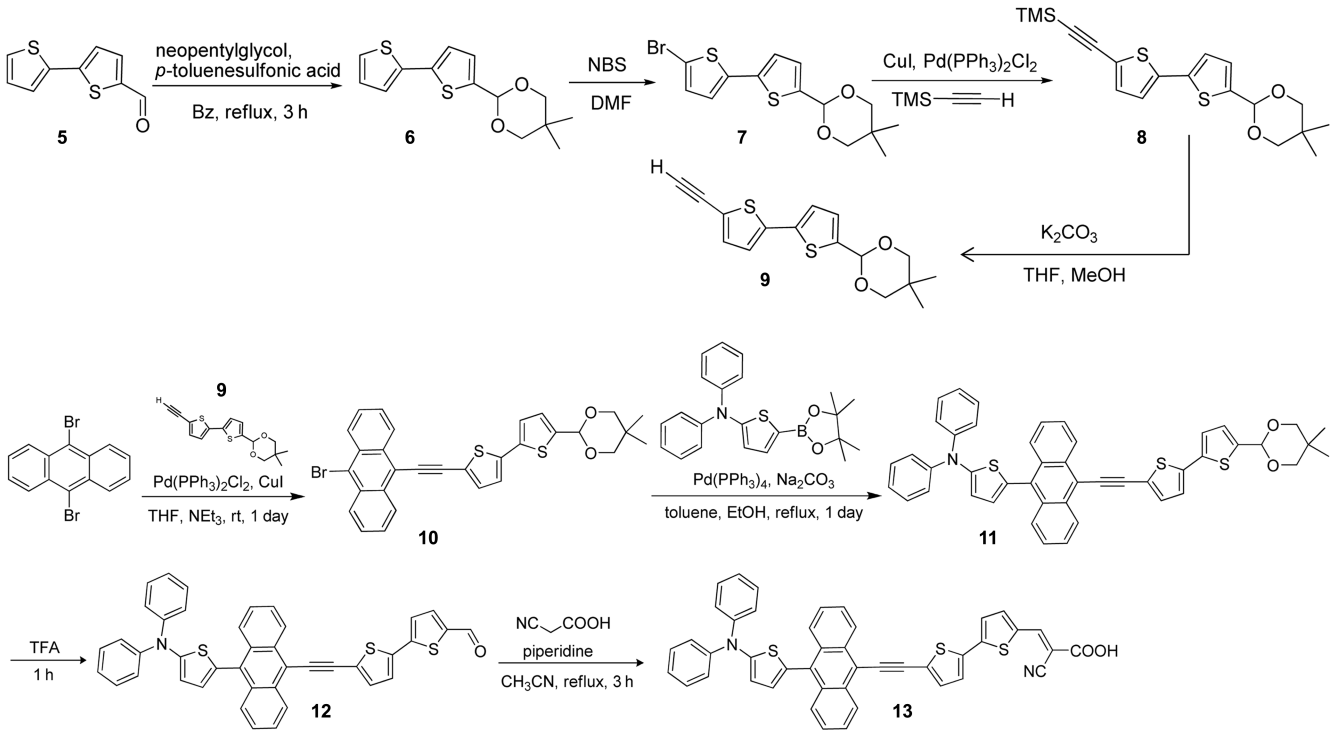

Scheme 2. Synthetic procedure for DPATABT, **13**.

compound **3** as a yellowish red solid (0.69 g, yield 74%).

^{1}H NMR (400 MHz, $CDCl_3$) δ 9.93 (s, 1H), 8.59 (d, J = 8.60 Hz, 2H), 8.11 (d, J = 8.60 Hz, 2H), 7.77 (d, J = 3.92 Hz, 1H), 7.66 (t, J = 7.04 Hz, 2H), 7.55 (t, J = 6.68 Hz, 2H), 7.53 (d, J = 3.92 Hz, 1H), 7.36-7.29 (m, 8H), 7.10 (t, J = 7.04 Hz, 2H), 6.97 (d, J = 3.92 Hz, 1H), 6.89 (d, J = 3.92 Hz, 1H). LRMS (*m/z*): [M^+] calcd for $C_{37}H_{23}NOS_2$, 561.12; found, 561.08. Anal. Calcd for $C_{37}H_{23}NOS_2$: C, 79.11; H, 4.13; N, 2.49; S, 11.42, found, C, 74.74; H, 3.75; N, 2.12; S, 10.98.

(*E*)-2-Cyano-3-(5-((10-(5-(diphenylamino)thiophen-2-yl)anthracen-9-yl)ethynyl)thiophen-2-yl)acrylic acid (4, DPATAT): Compound **3** (0.50 g, 0.89 mmol) and cynaoacetic acid (0.379 g, 4.45 mmol) were dissolved in acetonitrile (60 mL) and the solution was refluxed in the presence of a catalytic amount of piperidine (0.4 mL) for 8 h. After removing the solvent under vacuum, the residue was purified by silica-gel column chromatography (MC:methanol (10:1, v/v)) to give the pure DPATAT as a red solid (0.15 g, yield 26%).

^{1}H NMR (300 MHz, $CDCl_3$) δ 8.54 (d, J = 8.52 Hz, 2H), 8.14 (s, 1H), 7.99 (d, J = 8.52 Hz, 2H), 7.82-7.78 (m, 2H), 7.73 (m, 2H), 7.66 (d, J = 6.60 Hz, 1H), 7.63 (d, J = 6.60 Hz, 1H), 7.38 (t, J = 7.41 Hz, 8H), 7.21 (d, J = 7.41 Hz, 4H), 7.10 (d, J = 6.06 Hz, 1H), 7.09 (d, J = 6.06 Hz, 1H). LRMS (*m/z*): [M^+] calcd for $C_{40}H_{24}N_2O_2S_2$, 628.13; found, 628.14. Anal. Calcd for $C_{40}H_{24}N_2O_2S_2$: C, 76.41; H, 3.85; N, 4.46; S, 10.20, found, C, 75.55; H, 3.64; N, 4.32; S, 9.91.

2-(2,2'-Bithiophen-5-yl)-5,5-dimethyl-1,3-dioxane (6): 2,2'-Bithiophene-5-carbaldehyde (**5**) (5.0 g, 25.7 mmol), neopentylglycol (4.02 g, 38.6 mmol), and *p*-toluenesulfonic acid (0.48 g) were dissolved in benzene (50 mL). The reaction mixture was refluxed for 5 h and then, the cooled mixture was washed with aqueous sodium bicarbonate (5 wt %, 150 mL). The combined benzene layers were then dried with Na_2SO_4, filtered, and concentrated in vacuo to yield compound **6** as a white solid (4.5 g, 63%).

^{1}H NMR (300 MHz, DMSO-d_6) δ 7.20 (d, J = 5.22 Hz, 1H), 7.15 (d, J = 3.57 Hz, 1H), 7.04 (d, J = 3.84 Hz, 1H), 7.02 (d, J = 4.65 Hz, 1H), 7.00 (d, J = 3.57 Hz, 1H) 5.61 (s, 1H), 3.77 (d, J = 11.36 Hz, 2H), 3.65 (d, J = 11.36 Hz, 2H), 1.28 (s, 3H), 0.80 (s, 3H) LRMS (*m/z*): [M^+] calcd for $C_{14}H_{16}O_2S_2$, 280.41; found, 280.35. Anal. Calcd for $C_{14}H_{16}O_2S_2$: C, 59.97; H, 5.75; S, 22.87, found, C, 59.15; H, 5.22; S, 21.67.

2-(5'-Bromo-2,2'-bithiophen-5-yl)-5,5-dimethyl-1,3-dioxane (7): The compound **6** (4.5 g, 16.0 mmol) was dissolved in DMF (35 mL) and NBS (3.43 g, 19.3 mmol) in DMF (5 mL) was added into the mother solution dropwise over 30 min. The solution was allowed to stir for 5 h. The mixture was poured into water and the separated organic layer was dried with Na_2SO_4, and concentrated under vacuum. The crude product was purified by silica-gel column chromatography (MC:hexane = 1:2 (v/v)). Pure solid product of compound **7** was obtained (3.5 g, 61%).

^{1}H NMR (300 MHz, $CDCl_3$) δ 7.01 (d, J = 3.84 Hz, 1H), 6.97 (d, J = 4.11 Hz, 1H), 6.95 (d, J = 4.11 Hz, 1H), 6.89 (d, J = 3.84 Hz, 1H) 5.61 (s, 1H), 3.77 (d, J = 11.36 Hz, 2H), 3.65 (d, J = 11.36 Hz, 2H), 1.28 (s, 3H), 0.80 (s, 3H). LRMS (*m/z*): [M^+] calcd for $C_{14}H_{15}BrO_2S_2$, 357.97; found, 358.01. Anal. Calcd for $C_{14}H_{15}BrO_2S_2$: C, 46.80; H, 4.21; S, 17.85, found, C, 45.62; H, 4.15; S, 17.34.

((5'-(5,5-Dimethyl-1,3-dioxan-2-yl)-2,2'-bithiophen-5-yl)ethynyl)trimethylsilane (8): Compound **7** (6.2 g, 17.3 mmol) was dissolved in a THF solution (100 mL) of $PdCl_2(PPh_3)_2$ (0.6 g, 0.086 mmol) and CuI (0.16 g, 0.086 mmol), followed by adding, trimethylsilyl acetylene (2.54 g, 25.9 mmol), diisopropylamine (15 mL), and triethylamine (20 mL). The resulting mixture was allowed to stir for 24 h at room temperature. The dark solution was concentrated and the resulting black solid was extracted with MC. Further purification was performed by silica-gel chromatography with MC:hexane (1:2 v/v) to give compound **8** as a white solid (5.19 g, 80%).

^{1}H NMR (400 MHz, $CDCl_3$) δ 7.11 (d, J = 3.92 Hz, 1H), 7.05 (d, J = 3.52 Hz, 1H), 7.03 (d, J = 4.32 Hz, 1H), 6.99 (d, J = 3.92 Hz, 1H), 5.61 (s, 1H), 3.77 (d, J = 11.36 Hz, 2H), 3.65 (d, J = 11.36 Hz, 2H), 1.28 (s, 3H), 0.80 (s, 3H), 0.25 (s, 9H). LRMS (*m/z*): [M^+] calcd for $C_{19}H_{24}O_2S_2Si$, 376.10; found, 376.25. Anal. Calcd for $C_{19}H_{24}O_2S_2Si$: C, 60.59; H, 6.42; S, 17.03, found, C, 62.10; H, 6.50; S, 16.49.

2-(5'-Ethynyl-2,2'-bithiophen-5-yl)-5,5-dimethyl-1,3-dioxane (9): To a stirred solution of compound **8** (5.3 g, 14.1 mmol) in THF (30 mL) and methanol (90 mL) was added K_2CO_3 (5.83 g, 42.2 mmol). The mixture was allowed to stir for 24 h at room temperature and concentrated in vacuo. The residue was diluted with MC and washed with water. The organic phase was dried over Na_2SO_4, filtered, and concentrated under vacuum. The resulting organic compound was dissolved in MC and purified by a silica-gel column chromatography with MC to afford compound **9** as a white solid (3.8 g, 90%).

^{1}H NMR (400 MHz, $CDCl_3$) δ 7.16 (d, J = 3.92 Hz, 1H), 7.56 (d, J = 3.92 Hz, 1H), 7.03 (d, J = 3.92 Hz, 1H), 7.01 (d, J = 3.92 Hz, 1H), 5.61 (s, 1H), 3.77 (d, J = 11.36 Hz, 2H), 3.65 (d, J = 11.36 Hz, 2H), 1.28 (s, 3H), 0.80 (s, 3H). LRMS (*m/z*): [M^+] calcd for $C_{16}H_{16}O_2S_2$, 304.06; found, 304.11. Anal. Calcd for $C_{16}H_{16}O_2S_2$: C, 63.13; H, 5.30; S, 21.07, found, C, 64.28; H, 5.19; S, 21.56.

2-(5'-((10-Bromoanthracen-9-yl)ethynyl)-2,2'-bithiophen-5-yl)-5,5-dimethyl-1,3-dioxane (10): To a mixture of $PdCl_2(PPh_3)_2$ (152 mg, 0.217 mmol) and CuI (41 mg, 0.217 mmol) in THF (300 mL) were added successively 9,10-dibromoanthracene (5.5 g, 16.3 mmol), compound **9** (3.3 g, 10.8 mmol), triethylamine (10 mL), and diisopropylamine (10 mL). The resulting mixture was stirred for 5 h at 60 °C. The dark solution was concentrated under vacuum and the resulting black solid was extracted with MC (3 × 50 mL) and further purified by silica-gel chromatography with MC: hexane (1:1 v/v) to give compound **10** as a yellow solid (1.2 g, 20%).

^{1}H NMR (400 MHz, DMSO-d_6) δ 8.61-8.55 (m, 4H), 7.65-7.62 (m, 4H), 7.39 (d, J = 3.92 Hz, 1H), 7.16 (d, J = 3.52 Hz, 1H), 7.14 (d, J = 3.92 Hz, 1H), 7.08 (d, J = 4.28 Hz, 1H), 5.64 (s, 1H), 3.80 (d, J = 11.36 Hz, 2H), 3.68 (d, J =

11.36 Hz, 2H), 1.31 (s, 3H), 0.82 (s, 3H). LRMS (*m/z*): [M^+] calcd for $C_{30}H_{23}BrO_2S_2$, 558.03; found, 559.90. Anal. Calcd for $C_{30}H_{23}BrO_2S_2$: C, 64.40; H, 4.14; S, 11.46, found, C, 64.28; H, 4.23; S, 12.01.

5-(10-((5'-(5,5-Dimethyl-1,3-dioxan-2-yl)-2,2'-bithiophen-5-yl)ethynyl)anthracen-9-yl)-*N,N*-diphenylthiophen-2-amine (11): A procedure similar to that described for compound **3** was followed by using **10** instead of **1** to give **11** in 75% yield as a red powder (1.3 g).

^{1}H NMR (400 MHz, DMSO-d_6) δ 9.86 (s, 1H), 8.58 (d, *J* = 8.60 Hz, 2H), 8.08 (d, *J* = 8.64 Hz, 2H), 7.66 (d, *J* = 3.92 Hz, 1H), 7.60 (t, *J* = 7.44 Hz, 2H), 7.52 (t, *J* = 8.24 Hz, 2H), 7.41 (d, *J* = 3.92 Hz, 1H), 7.32 (m, 7H), 7.23 (s, 1H), 7.07 (t, *J* = 7.04 Hz, 2H), 6.94 (d, *J* = 3.52 Hz, 1H), 6.87 (d, *J* = 3.56 Hz, 1H). LRMS (*m/z*): [M^+] calcd for $C_{46}H_{35}NO_2S_3$, 729.18; found, 730.12. Anal. Calcd for $C_{46}H_{35}NO_2S_3$: C, 75.69; H, 4.83; N, 1.92; S, 13.18, found, C, 75.86; H, 4.79; N, 2.05; S, 13.56.

5'-((10-(5-(Diphenylamino)thiophen-2-yl)anthracen-9-yl)ethynyl)-2,2'-bithiophene-5-carbaldehyde (12): Compound **11** (1.25 g, 1.71 mmol) was dissolved in THF (80 mL) and water (20 mL). Trifluoroacetic acid (10 mL) was then added to the reaction mixture. The resulting reaction mixture was allowed to stir for 3 h at room temperature and carefully quenched with saturated aqueous solution of $NaHCO_3$ (aq) and the mixture was extracted with MC. The organic layer was separated and dried over $MgSO_4$. The solvent was removed from the mixture under vacuum. The crude product **12** was purified by silica-gel chromatography (eluent: MC) to yield 0.9 g (81%) of an orange powder.

^{1}H NMR (300 MHz, DMSO-d_6) δ 9.88 (s, 1H), 8.58 (d, *J* = 8.52 Hz, 2H), 8.07 (d, *J* = 8.76 Hz, 2H), 7.68 (d, *J* = 3.30 Hz, 1H), 7.62 (t, *J* = 6.87 Hz, 2H), 7.53 (t, *J* = 7.14 Hz, 2H), 7.42 (d, *J* = 3.57 Hz, 2H), 7.31 (m, 10H), 7.08 (t, *J* = 6.87 Hz, 2H), 6.95 (d, *J* = 2.73 Hz, 1H), 6.88 (d, *J* = 3.27 Hz, 1H). LRMS (*m/z*): [M^+] calcd for $C_{41}H_{25}NOS_3$, 643.11; found, 643.10. Anal. Calcd for $C_{41}H_{25}NOS_3$: C, 76.48; H, 3.91; N, 2.18; S, 14.94, found, C, 76.15; H, 3.91; N, 2.06; S, 16.21.

(*E*)-2-Cyano-3-(5'-((10-(5-(diphenylamino)thiophen-2-yl)anthracen-9-yl)ethynyl)-2,2'-bithiophen-5-yl)acrylic acid (13, DPATABT): A procedure similar to that described for compound **4** was followed by using **12** instead of **3** to give the dye **13** in 40% yield as a dark red powder. (0.5 g) ^{1}H NMR (300 MHz, DMSO-d_6) δ 8.55 (d, *J* = 8.79 Hz, 2H), 8.51 (s, 1H), 8.02 (d, *J* = 8.49 Hz, 2H), 7.99 (d, *J* = 4.26 Hz, 1H), 7.76 (d, *J* = 3.87 Hz, 1H), 7.72 (d, *J* = 8.52 Hz, 2H), 7.68 (d, *J* = 3.84 Hz, 1H), 7.65 (t, *J* = 8.52 Hz, 2H), 7.39 (t, *J* = 7.14 Hz, 4H), 2.23 (d, *J* = 7.41 Hz, 4H), 7.11 (t, *J* = 7.14 Hz, 2H), 7.09 (d, *J* = 3.84 Hz, 1H), 6.97 (d, *J* = 3.84 Hz, 1H). LRMS (*m/z*): [M^+] calcd for $C_{44}H_{26}N_2O_2S_3$, 710.12; found, 710.21. Anal. Calcd for $C_{44}H_{26}N_2O_2S_3$: C, 74.34; H, 3.69; N, 3.94; S, 13.53, found, C, 74.34; H, 3.72; N, 3.86; S, 13.58.

Instrumental Analysis. ^{1}H NMR spectra were recorded on a Varian Mercury NMR 400 and 300 MHz spectrometers using $CDCl_3$ and DMSO-d_6 purchased from Cambridge Isotope Laboratories, Inc. Elemental analyses were performed by the Center for Organic Reactions using an EA1112 (Thermo Electron Corp.) elemental analyzer. Low resolution mass analysis was performed on a JMS-700 MStation mass spectrometer (JEOL, resolution 60,000, *m/z* range at full sensitivity 2,400). Absorption spectra were obtained using a UV-vis spectrometer (HP 8453, PDA type) in the wavelength range of 190-1100 nm. Photoluminescence (PL) spectra were recorded with a Hitachi F-7000 FL spectrophotometer. The redox properties of the two dyes were examined by cyclic voltammetry (CV) conducted using a potentiostat (EA161, eDAQ). A 0.10 M tetrabutylammonium hexafluorophosphate (Bu_4NPF_6) solution in freshly dried DMF was employed as an electrolyte. The Ag/AgCl and Pt wire (0.5 mm in diameter) electrodes were utilized as reference and counter electrodes, respectively. The scan rate was 50 mV s^{-1}.

Assembly and Characterization of DSSCs. The fabrication method of DSSC is as follows. The conducting glass substrate (FTO; TEC8, Pilkington, 8 Ω/cm^2, Thickness of 2.3 mm) was cleaned in ethanol by ultrasonication. The TiO_2 pastes (TiO_2 particle size: *ca.* 20 nm) were prepared using ethyl cellulose, lauric acid, and terpineol. The prepared TiO_2 paste was coated onto the pre-cleaned glass substrate using a doctor blade and sintered at 500 °C for 30 min. The thickness of the sintered TiO_2 layer was measured with an Alpha-Step IQ surface profiler (KLA-Tencor). For dye adsorption, the thermally annealed TiO_2 electrodes were immersed in dye solution (0.5 mM of dye in DMF) at 50 °C for 3 h. Pt counter electrodes were prepared by thermal reduction of thin film formed from 7 mM of H_2PtCl_6 in 2-propanol at 400 °C for 20 min. The dye-adsorbed TiO_2 electrode and Pt counter electrode were assembled using 60 μm-thick Surlyn (Dupont 1702) as a bonding agent. A liquid electrolyte was introduced through a pre-punctured hole on the counter electrode. The electrolyte was composed of 3-propyl-1-methyl-imidazolium iodide (PMII, 0.7 M), LiI (0.2 M), I_2 (0.05 M), and *t*-butylpyridine (TBP, 0.5 M) in acetonitrile/valeronitrile (85:15 v/v). The active areas of dye-adsorbed TiO_2 films were estimated using a digital microscope camera with image-analysis software (Moticam 1000, Motic Group Co., Ltd.).

Results and Discussion

Synthesis of 5-(Anthracen-9-yl)-*N,N*-diphenylthiophen-2-amine-based Dyes. The synthetic procedures of the D-π-A-type anthracene-mediated dyes synthesized in this study are shown in Schemes 1 and 2. For preparing DPATAT **4**, Suzuki coupling method was employed to synthesize the compound **3** with **1** and **2** in the presence of tetrakistriphenylphosphine palladium (0). For preparing DPATABT, **13**, first, 2,2'-bithiophene-5-carbaldehyde, **5** was protected with neopentyl glycol to afford acetal 2-(2,2'-bithiophen-5-yl)-5,5-dimethyl-1,3-dioxane, **6**. After successful bromination of compound **6**, the palladium-catalyzed Sonogashira coupling reaction was adopted to prepare ((5'-(5,5-dimethyl-1,3-dioxan-2-yl)-2,2'-bithiophen-5-yl)ethynyl)trimethylsilane, **8** and deprotection was performed to yield the compound **9**. 2-

(5'-((10-Bromoanthracen-9-yl)ethynyl)-2,2'-bithiophen-5-yl)-5,5-dimethyl-1,3-dioxane, **10** was also prepared through Sonogashira coupling reaction with the compound **9** and 9,10-dibromoanthracene. The compound **10** was reacted with *N,N*-diphenyl-5-(4,4,5,5-tetramethyl-1,3,2-dioxaborolan-2-yl)thiophen-2-amine to give the compound **11** under Suzuki coupling conditions followed by deprotection reaction with trifluoroacetic acid yielding the compound **12**. Finally, Knoevenagel condensation of the aldehydes **3** and **12** with cyanoacetic acid was conducted in the presence of piperidine to give the two different photosensitizing dyes such as DPATAT, **4** and DPATABT, **13**.

Absorption and Photoluminescence (PL) Behaviors of New Photosensitizing Dyes. In DSSCs, photosensitizing dye is a unique component having a specific function of light harvesting. The spectral response of photosensitizer, overlapped with the solar emission will affect the photocurrent of the device; thus, we measured the UV-vis absorptions of the dyes, DPATAT and DPATABT both in ethanol solutions and adsorbed on TiO_2 surface. Figure 1 shows the UV/Vis absorption and PL emission spectra of DPATAT and DPATABT in ethanol solutions. The absorption spectrum of DPATAT shows a visible absorption bands at 442 and 469 nm (E_g^{opt} = 2.5 eV, ε = 33000 M^{-1} cm^{-1} at 469 nm) corresponding to the π-π* transitions in the conjugated molecules. The spectral properties of DPATABT are similar to those of DPATAT in solution states, although the former has a slightly longer absorption maximum wavelength (λ_{max}) and higher molar extinction coefficient (λ_{max} = 460 and 485 nm, E_g^{opt} = 2.39 eV, ε = 53000 M^{-1} cm^{-1} at 460 nm). Compared to DPATAT, the absorption spectrum of DPATABT is red-shifted by 16 nm owing to the introduction of bithiophene ring in the D-A linking group. The corresponding emission spectra were also observed; the PL spectrum of DPATABT showed slight bathochromic shift including the stronger emission shoulder at 620 nm, indicating stronger intermolecular interaction between DPATABT molecules.

Figure 2 shows absorption spectra of dye-adsorbed TiO_2 layers and a wider absorption range which is favourable to improve light-harvesting efficiency of DSSCs. When the dyes were tethered to the surface of TiO_2 nanoparticles, the absorption spectra shifted to a shorter or longer wavelength

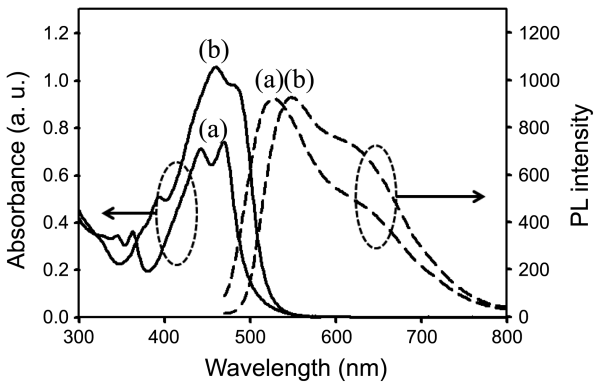

Figure 1. Absorption (solid line) and emission (dashed line) spectra of the two dyes in ethanol solution. (a) DPATAT, (b) DPATABT.

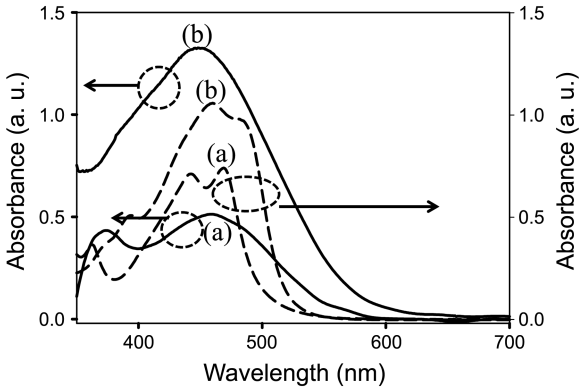

Figure 2. Absorption spectra of the two dyes adsorbed on TiO_2 layer. (a) DPATAT, (b) DPATABT (solid line). *Dashed lined-curves denotes the solution spectra of two dyes.

region as compared to that in the solution state because of mutual interaction between the dyes and the TiO_2 electrode surface, which results in a specific aggregated state of the dyes on TiO_2 surface.

The absorption peaks of DPATAT and DPATABT on TiO_2 electrodes were blue-shifted to 459 and 448 nm for dye-loaded TiO_2 layers (thickness ~2 μm). It can be seen that absorption spectra of the dyes on TiO_2 layers were blue-shifted slightly due to possible dissociation of π-π stacking or H-aggregation. The HOMO and LUMO energy levels are

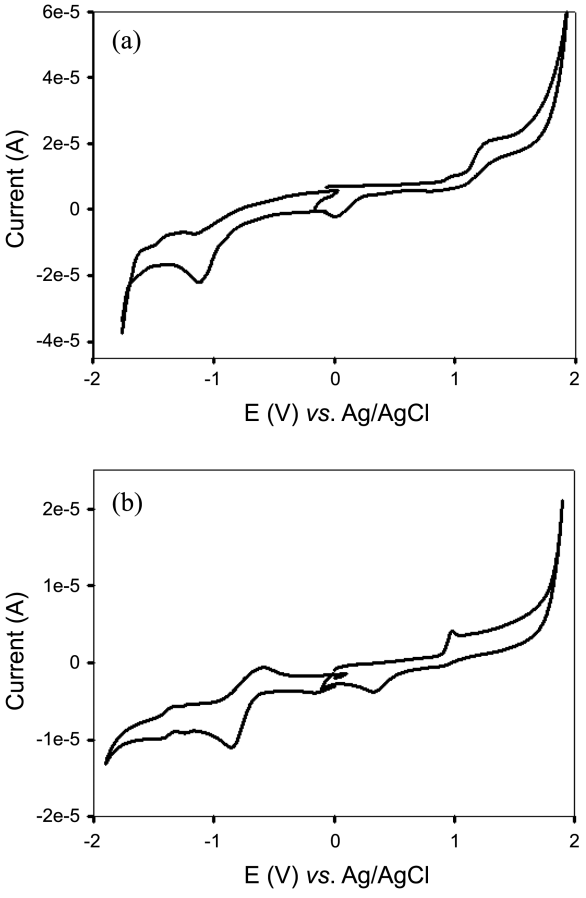

Figure 3. Cyclic voltammograms of (a) DPATAT and (b) DPATABT in DMF. [Standard $E_{ferrocene}^{onset}$ = 0.54 eV, E_g^{EC} = 1.6 eV (a), 1.57 eV (b)].

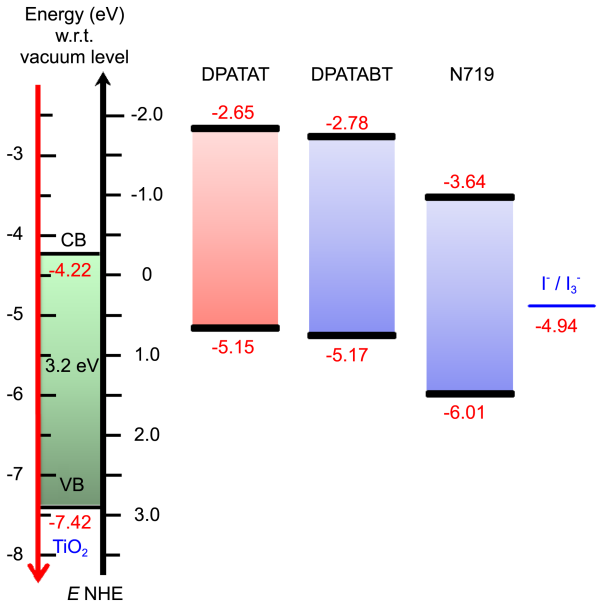

Figure 4. Energy diagram of DPATAT and DPATABT.

usually used to estimate the efficiency of electron injection from the dye in the photoexcited state to TiO_2 and the efficiency of dye regeneration. In a highly efficient DSSC, the LUMO energy of the dye molecule must be more shallow than that of the conduction band edge (–4.22 eV) in TiO_2. Effective electron injection from the excited dye molecules to the conduction band of the TiO_2 layer would be favorable. In order to induce effective regeneration of the dye molecules, the energy of the HOMO in the dye molecules should be deeper than the redox potential of I_3^-/I^-. The HOMO and LUMO energy levels of the dye molecules were measured by cyclic voltammetry (CV) and absorption spectroscopy, as shown in Table 1 and Figure 4.

Electrochemical Analysis of Two Photosensitizing Dyes. Cyclic voltammograms (CVs) were recorded in the DMF solution states of the dyes in dry DMF and the potentials were measured with respect to an internal reference such as ferrocene (F_c/F_c^+). (Figure 3) These CV scans showed reversible oxidation peaks in the range of –2.0 to +2.0 V (*vs.* Ag/AgCl). To determine the LUMO energy levels, we combined the oxidation potential obtained from CVs with the optical energy bandgap (E_g^{opt}) obtained from the absorption edge in the absorption spectrum (See Table 1).

The voltammograms of DPATAT and DPATABT in the solution states showed that their lowest HOMO energy levels appeared at –5.15 eV and –5.17 eV, respectively which are higher than that of I_3^-/I^- (–4.94 eV). Therefore, the oxidized dyes could be effectively regenerated using a redox electrolyte.

The E_{ox} values (0.89-0.91 V) of two anthracene-based dyes (Table 1) are sufficiently more negative than the potential of the I^-/I_3^-, indicating that the oxidized dyes accept electrons from I^- ions in the electrolyte after electron injection to TiO_2 electrode. The electrochemical LUMO levels of the dyes were calculated by E_{ox} - $E_{0\text{-}0}$, where $E_{0\text{-}0}$ is the zero-zero energy of the dyes. It was found that the values of E_{ox} - $E_{0\text{-}0}$ are more positive than the conduction band of TiO_2, thus the photoexcited dyes readily inject electrons to the conduction band of TiO_2. Thus, the bandgap energy of DPATABT was found to be smaller than that of DPATAT due to more extended π-conjugation length. Thus, the two dyes satisfy the requirements for reasonable performance of DSSCs. The energy level alignment diagram in DSSC devices was illustrated in Figure 4.

DSSC Devices Made of Two Photosensitizing Dyes. The newly synthesized organic dye photosensitizers were used to fabricate DSSCs to study their current density-voltage (*J-V*) characteristics. The photovoltaic properties of DSSCs made of DPATAT and DPATABT, were investigated under optimized fabrication conditions and standard global AM 1.5 solar conditions. The devices I and II were fabricated with the dyes DPATAT and DPATABT, respectively. The properties were compared with those of a DSSC containing N719 dye, as shown in Table 2. The cell did not contain a scattering layer and was not treated with $TiCl_4$. A moderately high PCE (η_{ave}) of 3.34 % (η_{max} = 3.7%) was achieved in the DSSC made of DPATABT with a relatively large active area of 0.41 cm^2. For the device I, the PCE value reached 2.05% with a short circuit current (J_{sc}) of 6.11 mA cm^{-2} and an open circuit voltage (V_{oc}) of 0.572 V. The lower PCE value is mainly due to the lower J_{sc} value (see Figure 5A). Extension of π-conjugated bridge by inserting a bithiophene unit into the structure of DPATABT led to an increase of photocurrent by 1.78 mA cm^{-2} compared to the device I.

The IPCE plots for the above-mentioned devices are also presented in Figure 5B. The photovoltaic responses of the devices I and II were quite similar to their absorption spectra; however, because of a higher molar extinction coefficient of DPATABT, it exhibited slightly higher IPCE around 68% at 460 nm as a result of more extended π-conjugation length. The lower extinction coefficient of DPATAT at 400-600 nm resulted in less absorption so that its external quantum efficiency (EQE) became lower than that of DPATABT. In the solar response range of 400-670 nm, the IPCE values of the device II were higher than those of the device I; thus, the

Table 1. Absorption, emission, and electrochemical properties of new photosensitizing dyes

Dye	λ_{max} [nm] (ε_{max} [10^4 M^{-1}·cm^{-1}])	λ_{em} [nm]	E_g^{opt} [eV]	$E_{0\text{-}0}$ [eV]	E_{ox}^{onset} [V]	HOMO [eV][a*]	LUMO [eV][b*]
DPATAT	442, 469 (3.3)	527	2.50	2.51	0.89	-5.15	-2.65
DPATABT	460, 485 (5.3)	548	2.39	2.43	0.91	-5.17	-2.78

[a]The values were determined by using E_{ox}^{onset} in cyclic voltammogram. [b]HOMO (eV) + E_g^{opt} (eV). *sample: solution in DMF. The optical bandgap was obtained from absorption spectrum of solution sample. $E_{ferrocene}^{onset}$ = 0.54 eV.

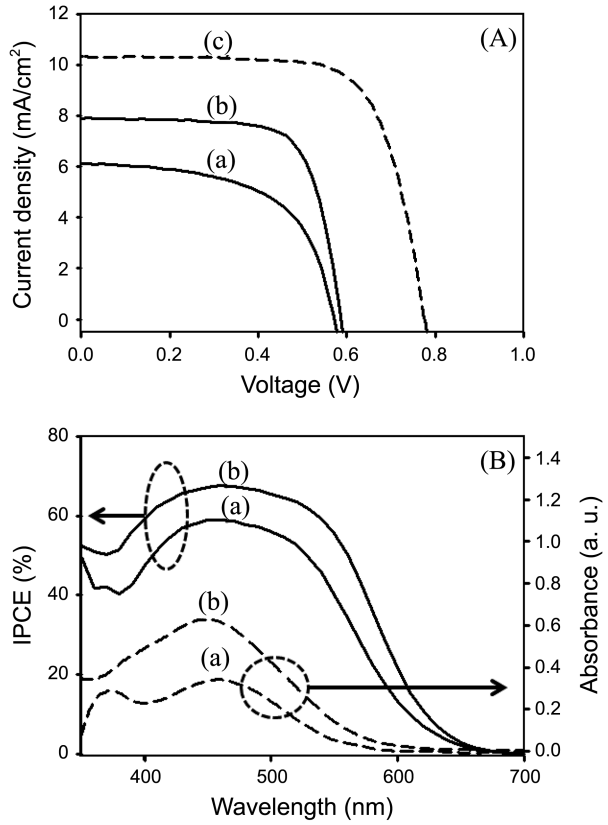

Figure 5. (A) *J-V* characteristics of DSSC with DPATAT (a) and DPATABT (b), and N719 (c). (B) Incident photon-to-current conversion efficiencies in DSSC with DPATAT (a) and DPATABT (b). *Dashed lined-curves denotes the corresponding absorption spectra of dye-adsorbed TiO_2 layers.

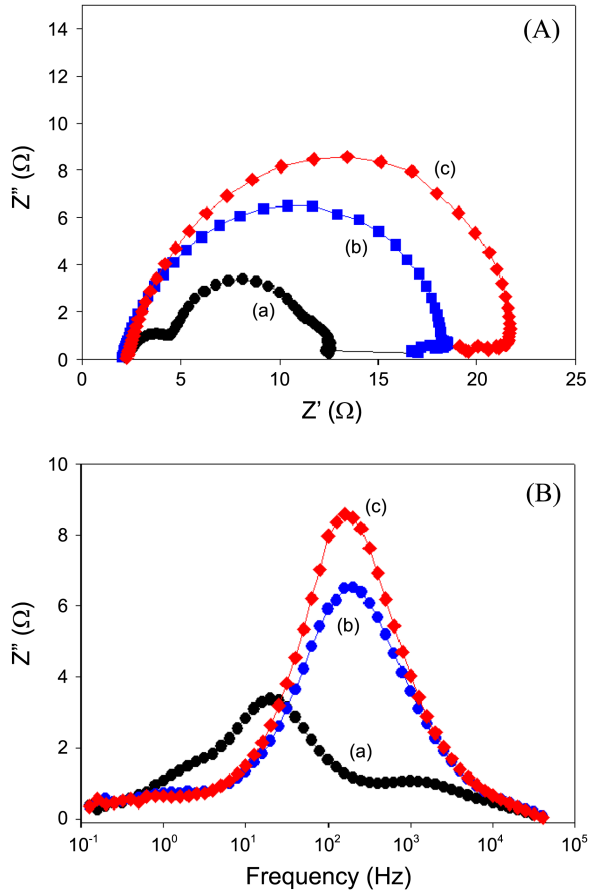

Figure 6. (A) Nyquist plots of the three DSSC cells at the light illumination. (a) circle: control device with N719; (b) square: device I; (c) diamond: device II. (B) The Bode plots for the three DSSC cells.

slightly higher EQE values observed for the device II mainly originated from the relatively large short-circuit photocurrent density and open circuit voltage. The DSSC characteristics of the dyes are improved upon incorporation of bithiophene segments into the conjugation pathway, which altered the HOMO and LUMO levels and subsequently favoured the electron-injection and recombination kinetics.

The small difference in the obtained open-circuit voltages (V_{oc} = 572-587 mV) could be attributed to different degree of adhesion of the dyes and the different electron pathways, resulting in modulation of resistance of electron transfer to the FTO interface. More importantly, the difference of V_{oc} can be the sign of enhanced recombination of charges at the TiO_2/dye/electrolyte interface. In order to understand the unique behavior of the electronic or ionic charge transport process in DSSC, electrochemical impedance spectroscopy (EIS) was carried out.[35] The variation of V_{oc} of DSSCs is influenced by possible charge transport properties, which can be investigated by EIS. It was performed to study the electrode kinetics and interfacial charge transfer process (TiO_2/dye/electrolyte) in the DSSCs. The precise analysis of the impedance variations in DSSCs composed of various organic photosensitizers allowed us to compare the electron life-times in three different DSSCs.[36]

We observed and analyzed the EIS under light illumination (100 mWcm^{-2}) conditions, as shown as Nyquist plots in Figure 6A. The recombination rate caused by the backward electron transfer was estimated by the Bode spectra for the DSSCs, as shown in Figure 6B. The electron life-times (τ_es) were calculated and are illustrated in Table 2. The peak shift from high frequency to low frequency reveals longer electron life-time because the frequency (f_{med}) can be related to the inverse of τ_e in TiO_2 films as ($\tau_e = 1/2\pi f_{med}$).[37,38] A

Table 2. Photovoltaic performances of DSSCs fabricated with anthracene-based dyes

Device	Dye	J_{sc} (mA cm^{-2})	V_{oc} (mV)	*FF* (%)	η (%)	EQE (%)	Life-time (ms)
Device I	DPATAT	6.11	572	58.5	2.05	59[a]	0.79
Device II	DPATABT	7.89	587	72.2	3.34	68[b]	1.00
Control device	N719	10.32	776	71.6	5.74	-	7.89

[a]λ = 450 nm. [b]λ = 460 nm

shorter electron life-time (τ_e = 0.79 ms) was obtained for the device I, compared with the longer life-time 1.00 ms for the device II, respectively. The results also supported the slightly larger V_{oc} of the device II, which indicates the longer electron life-time at the interface of TiO_2/dye/electrolyte.

Conclusion

D-π-A dyes containing anthracene units were successfully synthesized and showed promising properties as photosensitizers for use in DSSCs. Extending the π-conjugation length by introducing a bithiophene group significantly enhances the light-harvesting properties of the resulting compounds. The DPATABT-based DSSC showed the highest power conversion efficiency (PCE) of 3.34% under AM 1.5 illumination (100 mW cm^{-2}). The solar cell performance with DPATABT was found to be better than that of DPATAT-based DSSC.

Although the observed PCE values in the devices elaborated in this work were not very high, the anthracene-mediated conjugated dye was demonstrated to be a promising molecular frame for high-performance photosensitizing dyes.

Acknowledgments. This work was supported by the Korea Institute of Energy Technology Evaluation and Planning (KETEP) grant funded by the Ministry of Knowledge Economy under contract No. 20103020010010 and by Key Research Institute Program through the NRF funded by the Ministry of Education, Science and Technology (NRF20120005860).

References

1. O'Regan, B.; Grätzel, M. *Nature* **1991**, *353*, 737.
2. Grätzel, M. *Nature* **2001**, *414*, 338.
3. Nazeeruddin, M. K.; de Angelis, F.; Fantacci, S.; Selloni, A.; Viscardi, G.; Liska, P.; Ito, S.; Takeru, B.; Grätzel, M. *J. Am. Chem. Soc.* **2005**, *127*, 16835.
4. Yum, J.-H.; Jung, I.; Baik, C.; Ko, J.; Nazeeruddin, M. K.; Grätzel, M. *Energ. Environ. Sci.* **2009**, *2*, 100.
5. Gao, F.; Wang, Y.; Zhang, J.; Shi, D.; Wang, M.; Humphry-Baker, R.; Wang, P.; Zakeeruddin, S. M.; Grätzel, M. *Chem. Commun.* **2008**, 2635.
6. Horiuchi, T.; Miura, H.; Sumioka, K.; Uchida, S. *J. Am. Chem. Soc.* **2004**, *126*, 12218.
7. Wang, Z.-S.; Cui, Y.; Hara, K.; Dan-oh, Y.; Kasada, C.; Shinpo, A. *Adv. Mater.* **2007**, *19*, 1138.
8. Hara, K.; Wang, Z.-S.; Sato, T.; Furube, A.; Katoh, R.; Sugihara, H.; Dan-oh, Y.; Kasada, C.; Shinpo, A.; Suga, S. *J. Phys. Chem. B* **2005**, *109*, 15476.
9. Park, S. S.; Won, Y. S.; Choi, Y. C.; Kim, J. H. *Energy & Fuels* **2009**, *23*, 3732.
10. Tian, H.; Yang, X.; Cong, J.; Chen, R.; Liu, J.; Hao, Y.; Hagfeldt, A.; Sun, L. *Chem. Comm.* **2009**, 6288.
11. Tang, J.; Wu, W.; Hua, J.; Li, J.; Li, X.; Tian, H. *Chem. Comm.* **2009**, 982.
12. Khazraji, A. C.; Hotchandani, S.; Das, S.; Kamat, P. V. *J. Phys. Chem. B* **1997**, *103*, 4693.
13. Liang, M.; Xu, W.; Cai, F.; Chen, P.; Peng, B.; Chen, J.; Li, Z. *J. Phys. Chem. C* **2007**, *111*, 4465.
14. Hagberg, D. P.; Edvinsson, T.; Marinado, T.; Boschloo, G.; Hagfeldt, A.; Sun, L. *Chem. Commun.* **2006**, 2245.
15. Thomas, K. R. J.; Lin, J. T.; Hsu, Y.-C.; Ho, K.-C. *Chem. Comm.* **2005**, 4098.
16. Velusamy, M.; Thomas, K. R. J.; Lin, J. T.; Hsu, Y.-C.; Ho, K.-C. *Org. Lett.* **2005**, *7*, 1899.
17. Koumura, N.; Wang, Z.-S.; Mori, S.; Miyashita, M.; Suzuki, E.; Hara, K. *J. Am. Chem. Soc.* **2006**, *128*, 14256.
18. (a) Kim, S.; Lee, J. K.; Kang, S. O.; Ko, J.; Yum, J.-H.; Fantacci, S.; de Angelis, F.; Censo, D. D.; Nazeeruddin, M. K.; Grätzel, M. *J. Am. Chem. Soc.* **2006**, *128*, 16701. (b) Kozma, E.; Concina, I.; Braga, A.; Borgese, L.; Depero, L. E.; Vomiero, A.; Sberveglieri, G.; Catellani, M. *J. Mater. Chem.* **2011**, *21*, 13785.
19. Chen, C.-Y.; Wu, S.-J.; Wu, C.-G.; Chen, J.-G.; Ho, K.-C. *Angew. Chem. Int. Ed.* **2006**, *45*, 5822.
20. (a) Qin, P.; Yang, X.; Chen, R.; Sun, L.; Marinado, T.; Edvinsson, T.; Boschloo, G.; Hagfeldt, A. *J. Phys. Chem. C.* **2007**, *111*, 1853. (b) Fischer, M. K.; Wenger, S.; Wang, M.; Mishra, A.; Zakeeruddin, S. M.; Gratzel, M.; Bauerle, P. *Chem. Mater.* **2010**, *22*, 1836.
21. Tao, S.; Zhou, Y.; Lee, C. S.; Lee, S. T.; Huang, D.; Zhang, X. *J. Phys. Chem. C* **2008**, *112*, 14603.
22. Li, Z. H.; Wong, M. S.; Tao, Y.; Fukutani, H. *Org. Lett.* **2007**, *9*, 3659.
23. Liao, Y.-L.; Lin, C.-Y.; Wong, K.-T.; Hou, T.-H.; Hung, W.-Y. *Org. Lett.* **2007**, *9*, 4511.
24. Huang, T.-H.; Lin, J. T.; Chen, L.-Y.; Lin, Y.-T.; Wu, C.-C. *Adv. Mater.* **2006**, *18*, 602.
25. Xia, Z.-Y.; Zhang, Z.-Y.; Su, J.-H.; Zhang, Q.; Fung, K.-M.; Lam, M.-K.; Li, K.-F.; Wong, W.-Y.; Cheah, K.-W.; Tian, H.; Chen, C. H. *J. Mater. Chem.* **2010**, *20*, 3768.
26. Reddy, M. A.; Thomas, A.; Srinivas, K.; Rao, V. J.; Bhanuprakash, K.; Sridhar, B.; Kumar, A.; Kamalasanan, M. N.; Srivastava, R. *J. Mater. Chem.* **2009**, *19*, 6172.
27. Lyu, Y. Y.; Kwak, J.; Kwon, O.; Lee, S. H.; Kim, D.; Lee, C.; Char, K. *Adv. Mater.* **2008**, *20*, 2820.
28. Silvestri, F.; Marrocchi, A.; Seri, M.; Kim, C.; Marks, T. J.; Facchetti, A.; Taicchi, A. *J. Am. Chem. Soc.* **2010**, *132*, 6108.
29. Chung, D. S.; Park, J. W.; Park, J.-H.; Moon, D.; Kim, G. H.; Lee, H.-S.; Lee, D. H.; Shim, H.-K.; Kwon, S.-K.; Park, C. E. *J. Mater. Chem.* **2010**, *20*, 524.
30. Jung, K. H.; Bae, S. Y.; Kim, K. H.; Cho, M. J.; Lee, K.; Kim, Z. H.; Choi, D. H. *Chem. Commun.* **2009**, 5290.
31. Marrocchi, A.; Silvestri, F.; Seri, M.; Facchetti, A.; Taticchi, A.; Marks, T. J. *Chem. Commun.* **2009**, 1380.
32. Teng, C.; Yang, X. C.; Yang, C.; Li, S. F.; Cheng, M.; Hagfeldt, A.; Sun, L. *J. Phys. Chem. C* **2010**, *114*, 9101.
33. Srinivas, K.; Yesudas, K.; Bhanuprakash, K.; Rao, V. J.; Giribabu, L. *J. Phys. Chem. C* **2009**, *113*, 20117.
34. Thomas, K. R. J.; Singh, P.; Baheti, A.; Hsu, Y.-C.; Ho, K.-C.; Lin, J. T. *Dyes. Pigments* **2011**, *91*, 33.
35. (a) Kuang, D.; Ito, S.; Wenger, B.; Klein, C.; Moser, J. E.; Humphry-Baker, R.; Zakeerudddin, S. M.; Grätzel, M. *J. Am. Chem. Soc.* **2006**, *128*, 4146. (b) Kuang, D.; Wang, P.; Ito, S.; Zakeeruddin, S. M.; Grätzel, M. *J. Am. Chem. Soc.* **2006**, *128*, 7732. (c) Bisquert, J. *J. Phys. Chem. B* **2002**, *106*, 325. (d) Bisquert, J.; Zaban, A.; Greenshtein, M.; Mora-Sero, I. *J. Am. Chem. Soc.* **2004**, *126*, 13550.
36. Lee, K. M.; Suryanarayananb, V.; Ho, K. C. *J. Power Sources* **2009**, *188*, 635.
37. Sun, S.; Gao, L.; Liu, Y. *Appl. Phys. Lett.* **2010**, *96*, 083113.
38. Kern, R.; Sastrawan, R.; Ferber, J.; Stangl, R.; Luther, J. *Electrochim. Acta* **2002**, *47*, 4213.